Thermoeconomic assessment of a spectral-splitting hybrid PVT system in dairy farms for combined heat and power

Conference Paper · June 2019

Kai Wang
Zhejiang University

Antonio Marco Pantaleo
Università degli Studi di Bari Aldo Moro

María Herrando
University of Zaragoza

Ioannis Pesmazoglou
Solar Flow Ltd and Imperial College London

Thermoeconomic assessment of a spectral-splitting hybrid PVT system in dairy farms for combined heat and power

Kai Wang[a,*], Antonio Marco Pantaleo[a,b], María Herrando[c], Ioannis Pesmazoglou[d], Benjamin M. Franchetti[d] and Christos N. Markides[a]

[a] *Clean Energy Processes (CEP) Laboratory, Department of Chemical Engineering, Imperial College London, South Kensington Campus, London SW7 2AZ, United Kingdom*
[b] *Department of Agro-Environmental Sciences, University of Bari, Via Amendola 165/A, 70125 Bari, Italy*
[c] *Fluid Mechanics Group, University of Zaragoza, Zaragoza 50007, Spain*
[d] *Solar Flow Ltd., Imperial Innovations, 52 Princes Gate, London SW7 2PG, United Kingdom*
[*]*E-mail: kai.wang@imperial.ac.uk*

Abstract:

We investigate the thermoeconomic potential of a solar-combined heat and power (S-CHP) system based on concentrating, spectral-splitting hybrid photovoltaic-thermal (PVT) collectors for the provision of electricity, steam and hot water for processing milk products in dairy applications. Transient simulations are conducted by using a system model with real-time demand and weather data as inputs, taking account of the spectrum-selective features of the PV cells as well as key heat transfer mechanisms that determine the electrical and thermal performance of the PVT collector. Economic performance is also assessed by considering the investment and savings enabled by the reduced electrical and fuel consumption. The results show that incorporating spectral beam-splitting technology into hybrid PVT collectors can be effective in maintaining the PV cells at low temperatures, while at the same time supplying thermal outputs (fluid streams) at temperatures significantly higher than then cell temperatures for steam generation and/or hot water provision. Based on a 15,000-m^2 installed area, it is found that 80% of the thermal demand for steam generation and 60% of the hot water demand can be satisfied by the PVT S-CHP system, along with a net electrical output amounting to 60% of the demand. Economic and environmental assessments show that the system has an excellent decarbonisation potential (1,500 tCO_2/year) and is economically viable if the investment cost of the spectrum splitter is lower than 0.85 of the cost of the parabolic concentrator (i.e., <2,150 €/m^2 spectrum splitter) in this application.

Keywords:

CHP, combined heat and power, dairy, spectral splitting, PV, thermal, solar energy.

1. Introduction

Hybrid photovoltaic-thermal (PVT) system is an emerging solar combined heat and power (S-CHP) technology, which combines PV and solar thermal technologies in one component, allowing for electrical and thermal outputs generated simultaneously from the same installed area with a much higher overall efficiency if operated appropriately [1-4]. Previous studies have shown that PVT S-

CHP systems have promising thermoeconomic potentials in applications where both electricity and low-temperature heat are required, such as residential buildings [5,6], sports centres [7,8], university campuses [9], etc. However, as the PV module is thermally coupled with the heat transfer fluid and its electrical efficiency drops noticeably with the operating temperature (i.e., around −0.4%/°C for silicon solar cells), PVT systems are typically operated below 100 °C, which limits their applications in industries where higher temperature heat is often needed [10]. A promising solution to tackle this limitation is to split the incoming solar spectrum into two separate bands, one that is well-suited to conversion into electricity is directed to PV modules, and the rest that is absorbed as heat by a thermal absorber [11]. This decoupling of the thermal and electrical elements of the collector reduces the PV cell temperatures and allows higher electrical conversion efficiencies, while at the same time supplying a thermal output at temperatures considerably higher than the PV operation temperature.

Studies on spectral-splitting PVT collectors have focused mainly on thermal and optical characterisations of spectrum splitters [12-14], novel concept/prototype developments [15-17], and thermodynamic modelling at the component and system levels [18-20]. The thermal outputs of such PVT systems were explored for either generating additional electricity using power cycles [18,21,22] or providing relatively high-temperature heat [23-26]. Almost all existing modelling work is based on constant temperatures and flow rates predefined for the inlet heat transfer fluid, without any consideration of the coupling between thermal outputs and demands or their transient behaviour under intermittent solar or demand conditions. This can lead to significant under/overestimation of system performance, while also losing critical information on and insight into its dynamic operation.

In Europe, dairy is the most important sector within the food industry with regard to turnover [27]. Considerable amount of energy is required in the terms of heat and electricity in processing of milk and milk products. The required temperatures of thermal energy range from 60 °C to 200 °C for different heat treatment processes, such as pasteurization, sterilization, spray drying, etc [10,28]. Case studies for using solar processing heating systems in dairy industry were reported in literature [28-32], in which either parabolic trough collectors, flat plate thermal collectors or evacuated tube collectors are used, while PVT collectors have rarely been considered.

This work aims to investigate the thermoeconomic performance of a concentrating, spectral-splitting hybrid PVT S-CHP system in dairy farms. Transient simulations are conducted by using a system model with real-time demand and weather data as inputs, including a PVT collector model that accounts for the key optical and heat transfer mechanisms that determine its electrical and thermal performance. The potential of such spectral-splitting PVT systems are then assessed in terms of energetic, economic and environmental metrics.

2. Description of the spectral-splitting PVT system

The dairy farm considered in this work is a representative of a medium size factory in Bari, Italy with the monthly and hourly energy demand curves shown in Figure 1. The electrical and thermal demands are strongly hour- and month-dependent [29]. The farm requires two streams of thermal demands, which are supplied by steam and hot water, as denoted by $Q_{\mathrm{dem,h}}$ and $Q_{\mathrm{dem,l}}$ respectively. Steam at 152 °C and 5 bar is used as the heat transfer fluid for processing milk products while hot water is delivered at 60 °C for cleaning purposes in the farm. High thermal demands are required during winter, spring and summer as most of the milk production is done in these periods. The thermal demands reach the minimum in autumn as cheese production stops. High electrical demands, as denoted by P_{dem}, occur in summer due to the heavy loads for refrigeration.

The proposed hybrid S-CHP system for dairy farm applications is shown in Figure 2. It comprises PVT collectors, an oil tank for steam generation, a water tank for hot water provision, inverters and pumps. The PVT collectors use spectral-splitting designs similar to those in Ref. [26,33]. Solar radiation is reflected and concentrated by the full-spectral reflective parabolic mirror.

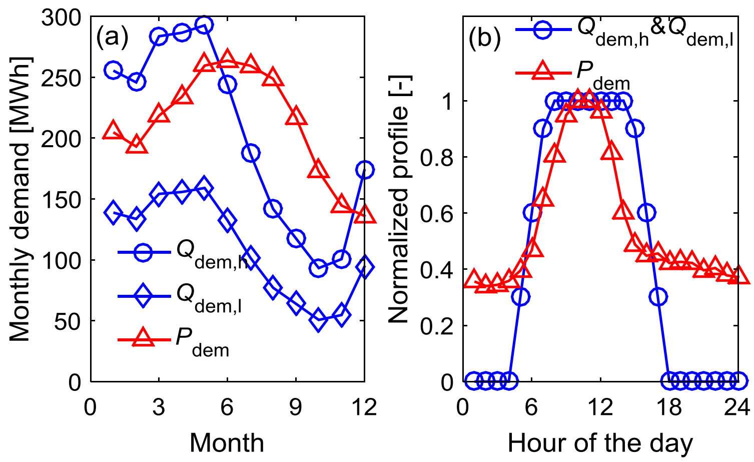

Figure 1. Energy demands of the dairy farm: (a) monthly thermal demand $Q_{dem,h}$ for steam generation, thermal demand $Q_{dem,l}$ for hot water and electrical demand P_{dem}; and (b) normalized hourly profiles of the thermal and electrical demands.

A portion of the concentrated solar radiation, which fits well with the spectrum requirement of the PV cells, is reflected by the spectrum splitters and redirected to the cells, while the rest passes through the splitter and is absorbed by the receivers for generating high-temperature oil. Water flowing in the water channels below the PV cells is used to cool the cells to ensure higher electrical conversion efficiency while generating low-temperature heat for hot water.

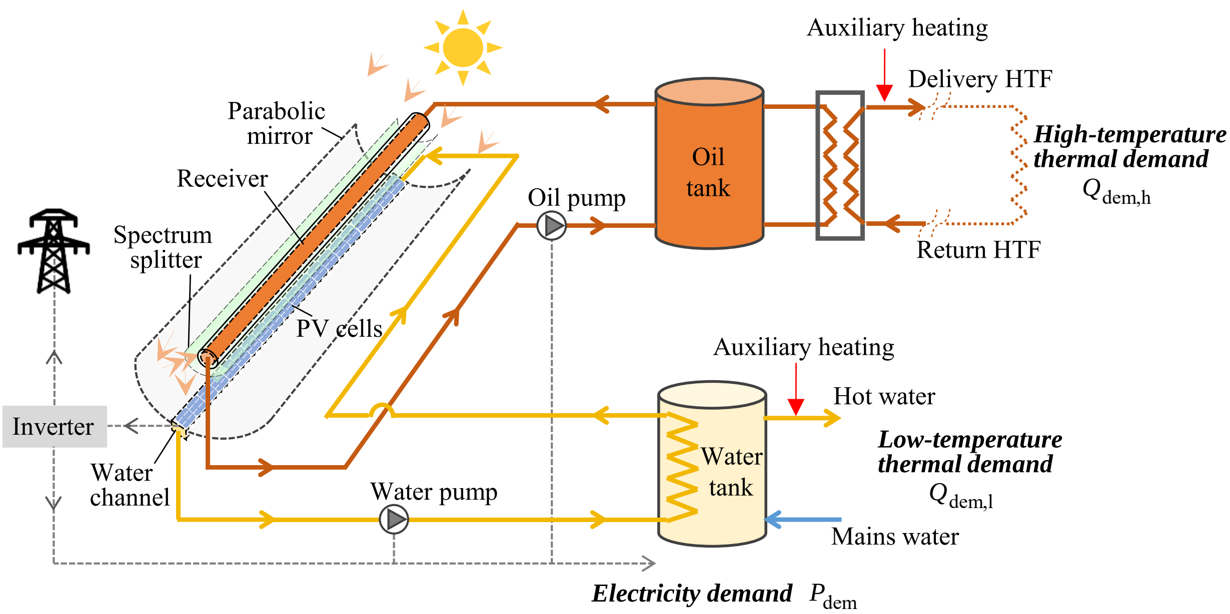

Figure 2. Schematic of a concentrating, spectral-splitting hybrid PVT system for combined heating and power provision to dairy applications.

Silicon solar cells with a spectral response curve given in Figure 3 are employed in this work. The spectral reflectance of the splitter determines how the solar radiance is allocated between the PV cells and receivers, which further influences the system thermoeconomic performance. A near-ideal spectrum splitter is assumed, as shown in Figure 3. It is highly reflective between 500 nm and 1100 nm while highly transparent for the rest of the solar spectrum. The absorptivity of the splitter is assumed as zero. The cut-off wavelengths have been optimised on the basis of the payback time for this dairy farm. The electricity generated from the PV cells is used to cover the electricity consumptions of the pumps and the electrical demand, and any surplus is exported to the electricity grid. Electricity is brought from the grid when the demand exceeds generation.

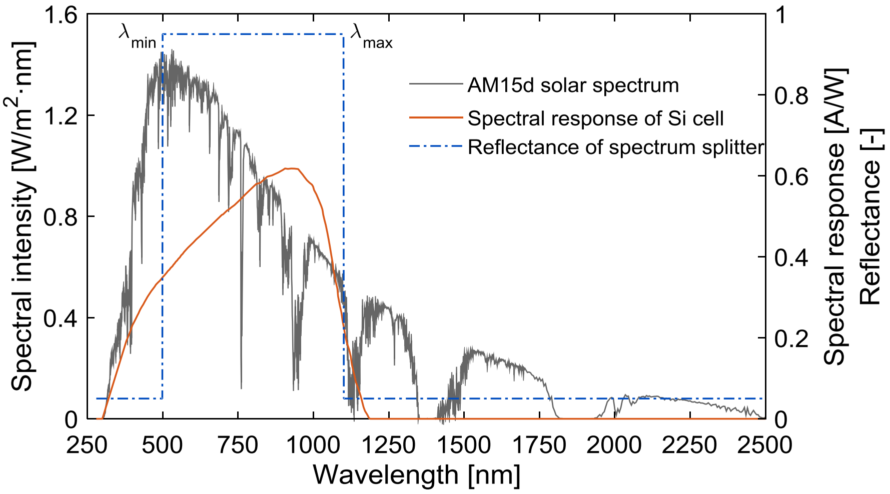

Figure 3. Solar spectrum, spectral response of Si-cell and reflectance of spectrum splitter.

3. Modelling methodology

A transient model has been built for the proposed spectral-splitting PVT system, which accounts for the key optical, electrical and heat transfer mechanisms that determine its electrical and thermal performance. The energy balance equations for the PV cells, water flow below the cells, and water in the water tank are expressed in Eqs. (1) – (3), respectively:

$$M_{\mathrm{pv}} C_{\mathrm{pv}} \frac{dT_{\mathrm{pv}}}{dt} = Q_{\mathrm{s,pv}} - Q_{\mathrm{r,pv-sky}} - Q_{\mathrm{c,pv-a}} - Q_{\mathrm{c,pv-w}} \tag{1}$$

$$\dot{m}_{\mathrm{w}} C_{\mathrm{w}} \left(T_{\mathrm{w,out}} - T_{\mathrm{w,in}} \right) = Q_{\mathrm{c,pv-w}} - Q_{\mathrm{r,w-sky}} - Q_{\mathrm{c,w-a}} \tag{2}$$

$$M_{\mathrm{wt}} C_{\mathrm{wt}} \frac{dT_{\mathrm{wt}}}{dt} = Q_{\mathrm{w-wt}} - Q_{\mathrm{wt,loss}} - Q_{\mathrm{dem,l}} \tag{3}$$

where M, C, T, Q and $\dot{m}$ denote the mass, heat capacity, temperature, heat transfer rate and mass flow rate, respectively. Q_{s}, Q_{r}, Q_{c} denote solar radiation, radiative heat transfer and connective heat transfer, respectively. $Q_{\mathrm{w-wt}}$, $Q_{\mathrm{wt,loss}}$ and $Q_{\mathrm{dem,l}}$ represent the rate of energy charged to the water tank, heat losses and the low-temperature thermal demand. The detailed equations for these heat transfer mechanisms can be found in Ref. [1] and Ref. [34].

The solar radiation $Q_{\mathrm{s,pv}}$ reaching the PV cells is calculated by integrating the reflectance $R(\lambda)$ of the spectrum splitter with the solar spectral intensity $I(\lambda)$ over the solar spectrum (λ = 280 – 4,000 nm),

$$Q_{\mathrm{s,pv}} = \left(1 - \eta_{\mathrm{pv}}\right) A_{\mathrm{PTC}} \eta_{\mathrm{PTC}} G / G_{\mathrm{AM1.5d}} \int_{280}^{4000} R(\lambda) I(\lambda)\, d\lambda \tag{4}$$

where η_{pv} and η_{PTC} are the electrical efficiency of the solar cells and the overall optical efficiency of the parabolic concentrator (0.8), respectively. $G/G_{\mathrm{AM1.5d}}$ is a ratio coefficient correcting the actual solar irradiation based on the air mass 1.5 (AM1.5d) condition. The profiles of $R(\lambda)$ and $I(\lambda)$ are given in Figure 3. The total aperture area (A_{PTC}) of the parabolic concentrator is set as 15,000 m^2, which is estimated based on the energy demands of the dairy farm. The electrical efficiency of the solar cells is calculated from,

$$\eta_{\mathrm{pv}} = \frac{V_{\mathrm{oc}} \cdot J_{\mathrm{sc}} \cdot FF}{A_{\mathrm{PTC}} \eta_{\mathrm{PTC}} G \cdot \left[\int_{280}^{4000} R(\lambda) I(\lambda)\, d\lambda / \int_{280}^{4000} I(\lambda)\, d\lambda \right]} \cdot \left[1 + \beta\left(T_{\mathrm{pv}} - T_{\mathrm{ref}}\right)\right] \tag{5}$$

where β and T_{ref} are the temperature coefficient (−0.45%/°C) and reference temperature (25 °C) of the cells, and V_{oc}, J_{sc} and FF are the open-circuit voltage, short-circuit current and filling factor. The equations for V_{oc} and FF are given in Ref. [23]. The short-circuit current is,

$$J_{\mathrm{sc}} = A_{\mathrm{PTC}} \eta_{\mathrm{PTC}} G / G_{\mathrm{AM1.5d}} \int_{280}^{4000} SR(\lambda) R(\lambda) I(\lambda)\, d\lambda \tag{6}$$

where $SR(\lambda)$ is the spectral response of the cells, as shown in Figure 3.

The energy balance equations for the glass cover of the receiver, absorber tube, thermal oil passing through the receiver tube and thermal oil in the oil tank are given in Eqs. (7) – (10), respectively.

$$M_{\mathrm{g}} C_{\mathrm{g}} \frac{dT_{\mathrm{g}}}{dt} = Q_{\mathrm{s,g}} + Q_{\mathrm{r,abt-g}} - Q_{\mathrm{r,g-sky}} - Q_{\mathrm{c,g-a}} \tag{7}$$

$$M_{\mathrm{abt}} C_{\mathrm{abt}} \frac{dT_{\mathrm{abt}}}{dt} = Q_{\mathrm{s,abt}} - Q_{\mathrm{r,abt-g}} - Q_{\mathrm{c,abt-o}} \tag{8}$$

$$Q_{\mathrm{c,abt-o}} = \dot{m}_{\mathrm{o}} C_{\mathrm{o}} \left(T_{\mathrm{o,out}} - T_{\mathrm{ot}}\right) = h_{\mathrm{abt}} A_{\mathrm{abt}} \left(T_{\mathrm{abt}} - T_{\mathrm{o,avg}}\right) \tag{9}$$

$$M_{\mathrm{ot}} C_{\mathrm{ot}} \frac{dT_{\mathrm{ot}}}{dt} = Q_{\mathrm{c,abt-o}} - Q_{\mathrm{ot,loss}} - Q_{\mathrm{dem,h}} \tag{10}$$

The solar energy absorbed by the glass cover $Q_{\mathrm{s,g}}$ and absorber tube $Q_{\mathrm{s,abt}}$ are calculated by,

$$Q_{\mathrm{s,g}} = \alpha_{\mathrm{g}} A_{\mathrm{PTC}} \eta_{\mathrm{PTC}} G / G_{\mathrm{AM1.5d}} \int_{280}^{4000} [1 - R(\lambda)] I(\lambda)\, d\lambda \tag{11}$$

$$Q_{\mathrm{s,abt}} = \alpha_{\mathrm{abt}} \tau_{\mathrm{g}} A_{\mathrm{PTC}} \eta_{\mathrm{PTC}} G / G_{\mathrm{AM1.5d}} \int_{280}^{4000} [1 - R(\lambda)] I(\lambda)\, d\lambda \tag{12}$$

where α_{g} and τ_{g} denote the average absorptivity and transmissivity of the glass, and α_{abt} is the average absorptivity of the absorber tube.

With given initial temperature conditions, weather conditions and demand data, Eqs. (1) – (3) and (7) – (10) are solved iteratively in MATLAB with a time step of an hour over the whole year.

Economic analyses are conducted in terms of payback time (*PBT*) and levelised cost of energy (*LCOE*), considering the system's investment cost, operation and maintenance costs, and cost savings due to the reduced natural gas and electricity bills required to satisfy the application's energy demand.

The annual cost saving, C_{s}, is calculated by,

$$C_{\mathrm{s}} = E_{\mathrm{cov}} \cdot c_{\mathrm{e}} + E_{\mathrm{exp}} \cdot s_{\mathrm{e}} + \frac{Q_{\mathrm{cov}}}{\eta_{\mathrm{boiler}}} c_{\mathrm{ng}} - C_{\mathrm{O\&M}} \tag{13}$$

where E_{cov} and Q_{cov} are the electrical and thermal demands covered by the system, E_{exp} the electricity exported to the grid via net metering, c_{e} and c_{ng} the prices for electricity (0.205 €/kWh) and natural gas (0.056 €/kWh) respectively, η_{boiler} the boiler efficiency (0.8), s_{e} the electricity price for the net metering option applicable to the system (0.103 €/kWh), and $C_{\text{O\&M}}$ the operation and maintenance (O&M) costs. The cost breakdowns for the spectral-splitting PVT S-CHP system are given in Table 1. As there is no available cost models for the spectrum splitter, its cost is assumed by using a range of fractions (0.05 – 1) of the parabolic concentrator.

Table 1. Cost breakdown of the spectral-splitting PVT S-CHP system.

Component	**Cost**
PV [€/kWp]	1000 [35]
Inverter [€/kW]	200 [35]
Water tank [€]	$0.874 \cdot V_{\text{t}}$ (l)+763.5 [36]
Pump [€]	$500 \cdot (P_{\text{pump}}/300)^{0.25}$ [37]
Piping [€]	$(0.897+0.21 \cdot d_{\text{pipe}}) \cdot L_{\text{pipe}}$ [37]
Controller [€]	500 [37]
Parabolic concentrator [€]	$185 \cdot A_{\text{PTC}}$ [38]
Oil tank [€]	$682 \cdot V_{\text{ot}}$ [38]
Spectrum splitter [€]	$(0.05 - 1) \cdot C_{\text{PTC}}$
Installation cost [€]	0.2·total component cost [37]
Annual O&M cost [€]	0.02·total component cost

The payback time, *PBT*, is calculated from,

$$PBT = \frac{\ln\left[\frac{C_0(i_{\text{F}} - d)}{C_{\text{s}}} + 1\right]}{\ln\left(\frac{1 + i_{\text{F}}}{1 + d}\right)} \tag{14}$$

where d is the discount rate (2.8%) and i_{F} the inflation rate (1.2%) assumed for the annual fuel savings. The levelised cost of energy, *LCOE*, is obtained by,

$$LCOE = \frac{C_0 + \sum_{i=1}^{n} C_{\text{O\&M}}(1 + i_{\text{F}})^{i-1}(1 + d)^{-i}}{\sum_{i=1}^{n} Q(1 + d)^{-i}} \tag{15}$$

where Q is the net annual production of energy in the form of electricity. As both thermal energy and electricity are provided from the PVT system, a conversion factor of 0.55 is used from thermal energy to electricity, which corresponds to the typical efficiency of a modern natural gas power plant [39]. The lifetime n is assumed as 25 years. The annual CO_2 emission reduction by the spectral-splitting PVT S-CHP system is also estimated based on the current CO_2 emission factors in Italy.

4. Results and discussion

Hourly transient simulations have been performed over the whole year in Bari of Italy with the weather and demand data given as inputs. The sizes of the oil and water tanks have been optimised based on the payback time and are selected as 300 m^3 and 150 m^3 respectively for the total solar field area of 15,000 m^2. The solar irradiance and the dynamic temperatures of the absorber tube of the receiver, oil tank, PV cells and water tank are shown in Figure 4. The overall profiles of the temperatures match with that of the solar irradiance, i.e., high solar irradiance leads to significant increases of the temperatures while low solar irradiance causes noticeable temperature drops. The tank temperatures are much higher in late summer and autumn, as the solar irradiance is higher while the thermal demands are significantly lower than those in other periods of the year. It is observed that the temperatures of the PV cells and water tank are mostly below 100 °C, while the oil temperature is normally much higher than 100 °C and reaches up to 400 °C when solar irradiance is high. The annual average temperatures of water and oil in the tanks are 54 °C and 225 °C, respectively. This implies that the spectral-splitting effectively ensures that the PV cells are operated at low temperatures, which is beneficial for the electricity production and cells' lifetime, while a high-temperature thermal output is also available from the solar receiver which is thermally decoupled from the PV cells.

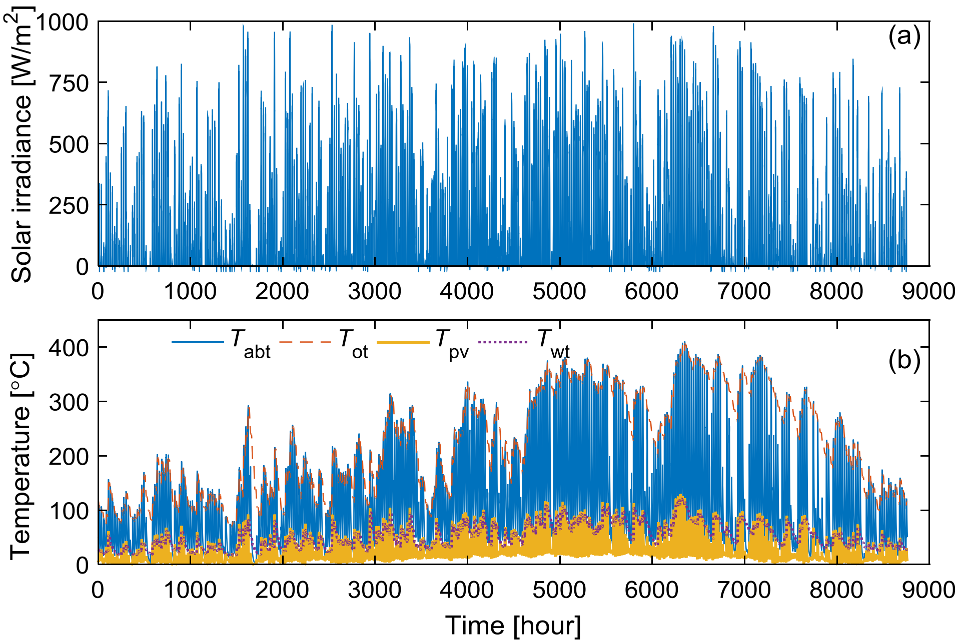

Figure 4. (a) Annual solar irradiance; and (b) temperature variations of the absorber tube of the receiver T_{abt}, oil tank T_{ot}, PV cell T_{pv} and water tank T_{wt}.

The detailed dynamic characteristics of the temperatures and electrical powers for typical five days in June are shown in Figure 5. When there is enough solar irradiance absorbed by the absorber tube and PV cells, their temperatures increase beyond the tank temperatures, as shown in Figure 5(a). The pumps are then triggered, circulating the fluids to deliver the collected thermal energy into the tanks for storage. When the solar irradiance is very low, the temperatures of the absorber tube and PV cells drops below the fluid temperatures in the tanks and thus the pumps are closed in this case. As shown in Figure 5(b), the electricity generated by the PVT system covers nearly all of the electrical demand at daytime, with the excess exported to the grid at high solar irradiances. As electricity storage is not considered in this work, the demand at night is thus completely met by the grid electricity.

Figure 6 shows summaries of the monthly energy demands and coverages. It is found that the proposed spectral-splitting PVT S-CHP system is able to cover most of the thermal demands, as shown in Figures 6(a) and (b). The coverage ratio for the thermal demand of steam generation is more than 80% from April to December. In particular, all the demands are covered from July to November. Due to the large thermal demand and low solar radiation from January to March, the coverage ratio is lower but still ranges from 50% to 70%. The thermal energy collected by the receiver covers 80% of the annual high-temperature thermal demands. Similar to the trends of the high-temperature thermal energy, most of the low-temperature thermal demand is covered in the periods from summer to autumn and the annual coverage ratio reaches 60%, as shown in Figure 6(b). The net electricity generation from the PV cells is 60% of the total electrical demand. Due to the mismatched daily profiles of solar energy and demand, 36% of the total electrical demand is directly covered, while the rest of net electricity is exported to the grid, as shown by the shadows denoted by P_{cov} and P_{exp}.

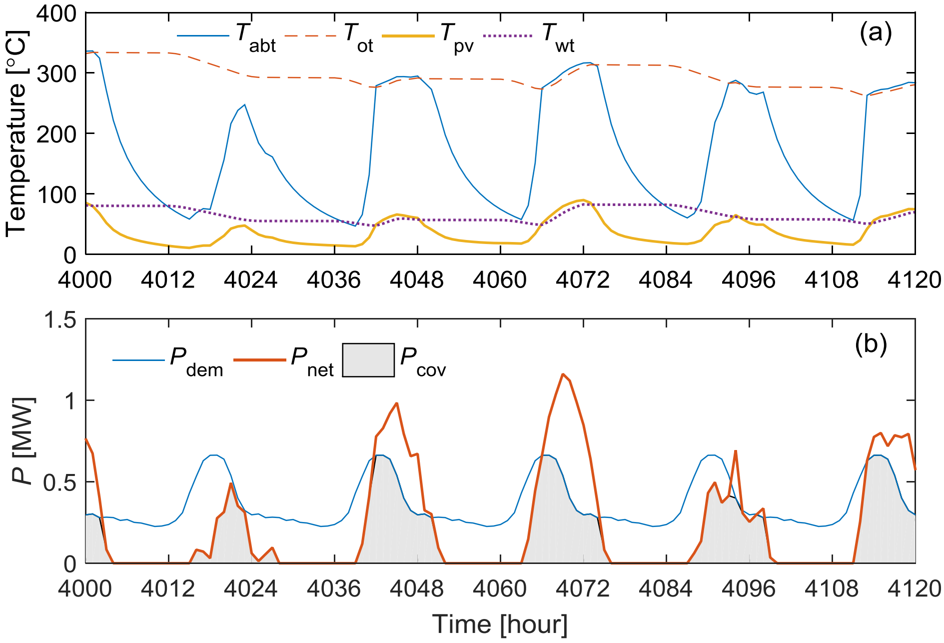

Figure 5. (a) Temperature variations of the absorber tube of the PTC receiver T_{abt}, oil tank T_{ot}, PV cell T_{pv} and water tank T_{wt}; and (b) variations of electrical demand P_{dem}, net electricity generation P_{net} and instantly covered electricity P_{cov}.

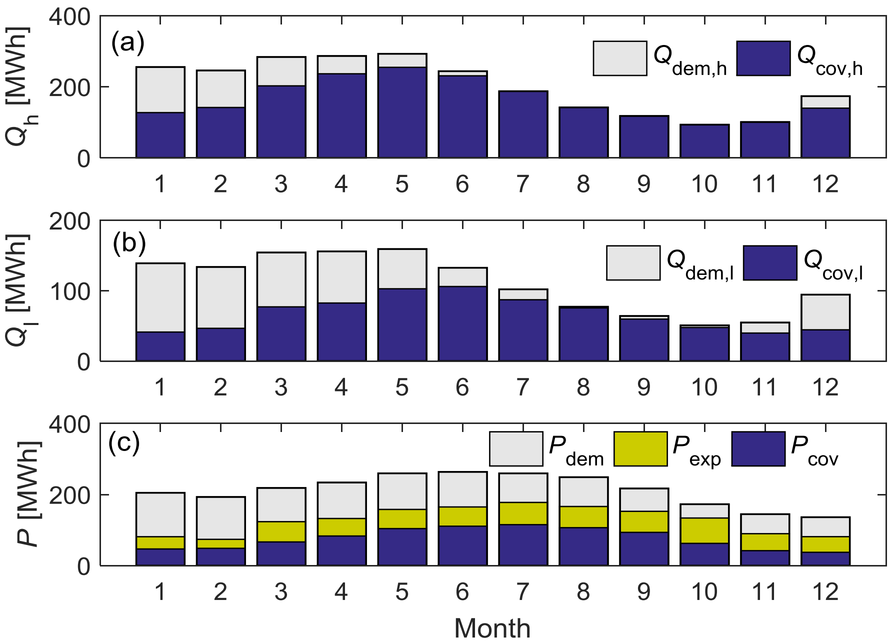

Figure 6. (a) High-temperature thermal demand $Q_{dem,h}$ and coverage $Q_{cov,h}$ for steam generation*; (b) low-temperature thermal demand $Q_{dem,l}$ and coverage $Q_{cov,l}$* for hot water*; and (c) electrical demand P_{dem}, net electricity generation P_{net} and instantly covered electricity P_{cov}.*

Based on the energy demand coverages obtained from the thermodynamic modelling, the economic performance of the PVT S-CHP system is further analysed. In particular, since the cost models for spectrum splitters are still not available, the possible range of investment cost of the spectrum splitter (C_{SS}) is estimated based on the total investment cost of the parabolic concentrator (C_{PTC}) which is a more established technology with relatively reliable cost estimations, as given in Table 1. Figure 7 shows the sensitivities of the payback time and levelised cost of energy to the cost of the spectrum splitter. It is found that the investment cost of the spectrum splitter should be less than 0.85 of the cost of the parabolic concentrator, in order to make the proposed PVT S-CHP system profitable, i.e., *PBT* < 25 years. The payback time ranges from 12.4 to 25 years when the splitter cost is 0.05 – 0.85 of the concentrator cost, which corresponds to about 130 – 2,150 € per unit area of the spectrum splitter. The levelised cost of energy is between 0.103 and 0.170 €/kWh for the splitter costs specified above.

Further incentives for renewable electricity and heating, and for high-efficiency cogeneration, are available from the White Certificates mechanism as operated in the Italian energy framework, which provides a contribution up to 250 €/TOE (ton oil equivalent) saved. These measures increase the profitability of investments proposed here, but have not been considered in this assessment. The CO_2 emission reduction is estimated at 1,500 tons/year, of which ~2/3 (960 tons) is associated with the reduced gas consumption for heating and the rest with the electricity generation. These findings suggest that the spectral-splitting PVT S-CHP system has an excellent decarbonisation potential, and is economically viable for dairy applications if the cost of the spectrum splitter is below 2,150 €/m^2.

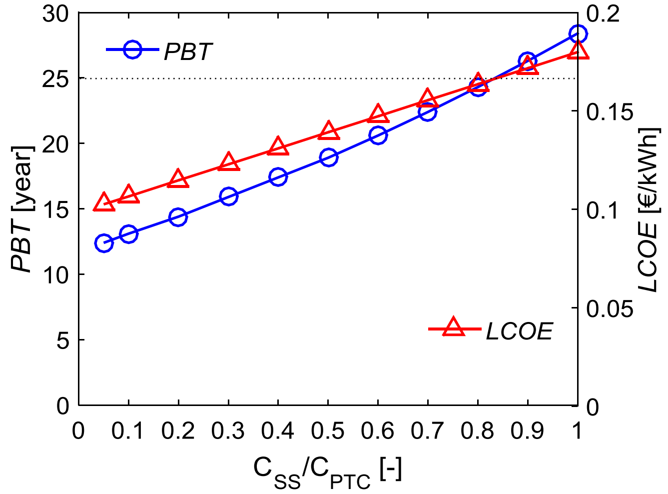

Figure 7. Sensitivity of payback time PBT and levelised cost of energy LCOE to the cost of the spectrum splitter C_{SS}/C_{PTC}.

5. Conclusion

A PVT S-CHP system has been studied for the provision of combined heat and power to dairy farms. The PVT collector is based on a parabolic-trough collector design, but with an additional spectrum splitter with which to separate the solar spectrum. The spectral band which is suitable for silicon PV is directed to the cells for electricity generation, while the rest is delivered to the absorber for steam production. The solar energy that is not converted into electricity by the PV cells is partially recovered by a water loop to provide hot water for the farm. A transient model has been developed, which accounts for the spectrum-selective features of the PVT collector and the various heat transfer mechanisms. Annual transient simulations have been performed with hourly weather and demand data as inputs. The results show that incorporating spectral-splitting technology effectively ensures that the PV cells are operated at relatively low temperatures (54 °C on average), which is beneficial for the electricity production and their lifetime, while the high-temperature thermal output is also simultaneously available from the solar receiver (225 °C on average). Based on an installed area of 15,000 m^2, the annual thermal energy produced by the PVT S-CHP system covers 80% of the thermal energy demand for steam production and 60% of hot water demand by the dairy farm. The net electricity generation of the S-CHP system reaches 60% of the total electrical demand, and 36% of the demand is instantly covered by the system with any excess exported to the grid. Economic analyses show that, in order to make the proposed system profitable within its lifetime, the investment cost of the spectrum splitter should be less than 0.85 of the cost of the parabolic concentrator in the proposed application, i.e., 2,150 € per unit area. The CO_2 emission reduction is estimated to be 1,500 tons/year, of which 960 tons originate from the reduced consumption of natural gas and the rest from the electricity. This work suggests that spectral-splitting PVT S-CHP systems have an excellent decarbonisation potential, and further efforts should be directed towards proposing spectrum-splitter designs with a cost that would make the system economically viable.

Acknowledgments

This work was supported by the UK Engineering and Physical Sciences Research Council (EPSRC) [grant number EP/M025012/1]. The authors would also like to thank UK company Solar Flow (www.solar-flow.co.uk). Data supporting this publication can be obtained on request from cep-lab@imperial.ac.uk.

Nomenclature

A	Area, m^2
c_e	Electricity price, €/kWh
c_{ng}	Natural gas price, €/kWh
C	Heat capacity, J/(kg·K)
C_0	Total cost, €
$C_{O\&M}$	Operation and maintenance costs, €
C_{PTC}	Cost of parabolic concentrator, €
C_s	Cost saving, €
C_{SS}	Cost of spectrum splitter, €
d	Discount rate
E_{cov}	Covered electricity, €
E_{exp}	Exported electricity, €
FF	Filling factor
G	Solar irradiance, W/m^2
h	Heat transfer coefficient, $W/(m^2 \cdot K)$
i_F	Inflation rate
I	Spectral intensity, $W/(m^2 \cdot nm)$
J	Current, A
$LCOE$	Levelised cost of energy, €/kWh
$\dot{m}$	Mass flow rate, kg/s
M	Mass, kg
n	Lifetime, year
PBT	Payback time, year
Q	Heat flow, W
Q_{cov}	Thermal energy covered, kWh
R	Reflectance
s_e	Electricity exporting price, €/kWh
SR	Spectral response, A/W
t	Time, s
T	Temperature, K
V	Voltage, V

Greek symbols

α	Absorptivity
β	Temperature coefficient, K^{-1}
η	Efficiency
λ	Wavelength, nm
τ	Transmissivity

Subscripts

a	Ambient
abt	Absorber tube
avg	Average
AM1.5d	Air-mass 1.5, direct
c	Convection
dem	Demand
g	Glass
h	High-temperature
in	Inlet
l	Low-temperature
loss	Thermal loss
o	Oil
oc	Open circuit
ot	Oil tank
out	Outlet
PTC	Parabolic trough concentrator
pv	PV cell
r	Radiation
ref	Reference
s	Solar radiation
sc	Short circuit
sky	Sky
w	Water
wt	Water tank

References

[1] Guarracino I., Mellor A., Ekins-Daukes N.J., Markides C.N, Dynamic coupled thermal-and-electrical modelling of sheet-and-tube hybrid photovoltaic/thermal (PVT) collectors. Appl Therm Eng 2016;101:778-95.

[2] Guarracino I., Freeman J., Ramos A., Kalogirou S.A., Ekins-Daukes N.J., Markides C.N., Systematic testing of hybrid PV-thermal (PVT) solar collectors in steady-state and dynamic outdoor conditions. Appl Energy 2019;240:1014-30.

[3] Mellor A., Alonso Alvarez D., Guarracino I., Ramos A., Riverola Lacasta A., Ferre Llin L., et al., Roadmap for the next-generation of hybrid photovoltaic-thermal solar energy collectors. Sol Energy 2018;174:386-98.

[4] Herrando M., Ramos A., Zabalza I., Markides C.N., A comprehensive assessment of alternative absorber-exchanger designs for hybrid PVT-water collectors. Appl Energy 2019;235:1583-602.

[5] Herrando M., Markides C.N., Hybrid PV and solar-thermal systems for domestic heat and power provision in the UK: Techno-economic considerations. Appl Energy 2016;161:512-32.

[6] Ramos A., Chatzopoulou M.A., Guarracino I., Freeman J., Markides C.N., Hybrid photovoltaic-thermal solar systems for combined heating, cooling and power provision in the urban environment. Energy Convers Manage 2017;150:838-50.

[7] Wang K., Herrando M., Pantaleo A.M., Markides C.N., Thermoeconomic assessment of a PV/T combined heating and power system for University Sport Centre of Bari. Energy Procedia. 2019.

[8] Wang K., Herrando M., Pantaleo A.M., Markides C.N., Thermodynamic and Economic Assessments of a Hybrid PVT-ORC Combined Heating and Power System for Swimming Pools. In: Riehl R.R., Preißinger M., Eames I.W., Tierney M., editors. HPC 2018: Proceedings of the 8th Heat Powered Cycles Conference; 2018 Sep 16-19; Bayreuth, Germany.

[9] Herrando M., Pantaleo A.M., Wang K., Markides C.N., Technoeconomic Assessment of a PVT-based Solar Combined Cooling Heating and Power (S-CCHP) System for the University Campus of Bari. In: The 13th Conference on Sustainable Development of Energy, Water and Environment Systems - SDEWES Conference; 2018 Sep 30-Oct 4; Palermo, Italy.

[10] Kalogirou S., The potential of solar industrial process heat applications. Appl Energy 2003;76:337-61.

[11] Joshi S.S., Dhoble A.S., Photovoltaic - Thermal systems (PVT): Technology review and future trends. Renew Sust Energy Rev 2018;92:848-82.

[12] Looser R., Vivar M., Everett V., Spectral characterisation and long-term performance analysis of various commercial heat transfer fluids (HTF) as direct-absorption filters for CPV-T beam-splitting applications. Appl Energy 2014;113:1496-511.

[13] Vivar M., Everett V., A review of optical and thermal transfer fluids used for optical adaptation or beam-splitting in concentrating solar systems. Prog Photovoltaics 2014;22:612-33.

[14] Crisostomo F., Taylor R.A., Zhang T., Perez-Wurfl I., Rosengarten G., Everett V., et al., Experimental testing of SiNx/SiO2 thin film filters for a concentrating solar hybrid PV/T collector. Renew Energy 2014;72:79-87.

[15] Mojiri A., Stanley C., Taylor R.A., Kalantar-zadeh K., Rosengarten G., A spectrally splitting photovoltaic-thermal hybrid receiver utilising direct absorption and wave interference light filtering. Sol Energy Mat Sol C 2015;139:71-80.

[16] Widyolar B., Jiang L., Abdelhamid M., Winston R., Design and modeling of a spectrum-splitting hybrid CSP-CPV parabolic trough using two-stage high concentration optics and dual junction InGaP/GaAs solar cells. Sol Energy 2018;165:75-84.

[17] Hangweirer M., Holler R., Schneider H., Design and analysis of a novel concentrated photovoltaic-thermal receiver concept. Jpn J Appl Phys 2015;54.

[18] Liu Y., Hu P., Zhang Q., Chen Z.S., Thermodynamic and optical analysis for a CPV/T hybrid system with beam splitter and fully tracked linear Fresnel reflector concentrator utilizing sloped panels. Sol Energy 2014;103:191-9.

[19] Brekke N., Dale J., DeJarnette D., Hari P., Orosz M., Roberts K., et al., Detailed performance model of a hybrid photovoltaic/thermal system utilizing selective spectral nanofluid absorption. Renew Energy 2018;123:683-93.

[20] Crisostomo F., Taylor R.A., Surjadi D., Mojiri A., Rosengarten G., Hawkes E.R., Spectral splitting strategy and optical model for the development of a concentrating hybrid PV/T collector. Appl Energy 2015;141:238-46.

[21] Branz H.M., Regan W., Gerst K.J., Borak J.B., Santori E.A., Hybrid solar converters for maximum exergy and inexpensive dispatchable electricity. Energ Environ Sci 2015;8:3083-91.

[22] Bierman D.M., Lenert A., Wang E.N., Spectral splitting optimization for high-efficiency solar photovoltaic and thermal power generation. Appl Phys Lett 2016;109.

[23] Ni J., Li J., An W., Zhu T., Performance analysis of nanofluid-based spectral splitting PV/T system in combined heating and power application. Appl Therm Eng 2018;129:1160-70.

[24] Zhao J.F., Song Y.C., Lam W.H., Liu W.G., Liu Y., Zhang Y., et al., Solar radiation transfer and performance analysis of an optimum photovoltaic/thermal system. Energ Convers Manage 2011;52:1343-53.

[25] Rodrigues F.M., Schaefer L.A., Long-term environmental impacts of a small-scale spectral filtering concentrated photovoltaic-thermal system. Energy Convers Manage 2019;184:350-61.

[26] Widyolar B., Jiang L., Winston R., Spectral beam splitting in hybrid PV/T parabolic trough systems for power generation. Appl Energy 2018;209:236-50.

[27] Ramirez C.A., Patel M., Blok K., From fluid milk to milk powder: Energy use and energy efficiency in the European dairy industry. Energy 2006;31:1984-2004.

[28] Sharma A.K., Sharma C., Mullick S.C., Kandpal T.C., Potential of solar industrial process heating in dairy industry in India and consequent carbon mitigation. J Clean Prod 2017;140:714-24.

[29] Cocco D., Tola V., Petrollese M., Application of concentrating solar technologies in the dairy sector for the combined production of heat and power. Energy Procedia 2016;101:1159-66.

[30] Sharma A.K., Sharma C., Mullick S.C., Kandpal T.C., Financial viability of solar industrial process heating and cost of carbon mitigation: A case of dairy industry in India. Sustain Energy Techn 2018;27:1-8.

[31] Quijera J.A., Alriols M.G., Labidi J., Integration of a solar thermal system in a dairy process. Renew Energy 2011;36:1843-53.

[32] Wallerand A.S., Kermani M., Voillat R., Kantor I., Marechal F., Optimal design of solar-assisted industrial processes considering heat pumping: Case study of a dairy. Renew Energy 2018;128:565-85.

[33] Jiang S.L., Hu P., Mo S.P., Chen Z.S., Optical modeling for a two-stage parabolic trough concentrating photovoltaic/thermal system using spectral beam splitting technology. Sol Energy Mat Sol C 2010;94:1686-96.

[34] Herrando M., Markides C.N., Hellgardt K., A UK-based assessment of hybrid PV and solar-thermal systems for domestic heating and power: System performance. Appl Energy 2014;122:288-309.

[35] Petrollese M., Cocco D., Optimal design of a hybrid CSP-PV plant for achieving the full dispatchability of solar energy power plants. Sol Energy 2016;137:477-89.

[36] Herrando M., Ramos A., Freeman J., Zabalza I., Markides C.N., Technoeconomic modelling and optimisation of solar combined heat and power systems based on flat-box PVT collectors for domestic applications. Energy Convers Manage 2018;175:67-85.

[37] Quoilin S., Declaye S., Tchanche B.F., Lemort V., Thermo-economic optimization of waste heat recovery organic Rankine cycles. Appl Therm Eng 2011;31:2885-93.

[38] Aguilar-Jiménez J.A., Velázquez N., Acuña A., Cota R., González E., González L., et al., Techno-economic analysis of a hybrid PV-CSP system with thermal energy storage applied to isolated microgrids. Sol Energy 2018;174:55-65.

[39] Gas Fired Power Plants, IEA Energy Technology Systems Analysis Programme - Technology Brief E02, 2010 – Available at: <https://iea-etsap.org/E-TechDS/PDF/E02-gas_fired_power-GS-AD-gct_FINAL.pdf> [accessed 11/01/2019].